

TEMPERATURE NON-UNIFORMITY DUE TO HEAT CONDUCTION AND RADIATION IN THE PULSE CALORIMETRY TECHNIQUE

by

Ivana D. NIKOLIĆ^{a*}, Nenad D. MILOŠEVIĆ^a, and Slobodan J. PETRIČEVIĆ^b

^a Vinča Institute of Nuclear Sciences - National Institute of the Republic of Serbia,
University of Belgrade, Belgrade, Serbia

^b School of Electrical Engineering, University of Belgrade, Belgrade, Serbia

Original scientific paper

<https://doi.org/10.2298/TSCI220115037N>

The paper presents an assessment of the unwanted temperature non-uniformity found in high temperature applications of the pulse calorimetry technique. Specimens in the form of a solid cylinder undergoes fast electrical heating and an intense heat radiation at high temperatures, coupled with the heat conduction the specimens' cold ends, make them having a highly non-uniform temperature distribution, both in their radial and axial directions. By using finite element method simulations of a typical pulse calorimetry experiment, the temperature non-uniformity across the specimen diameter and along the specimen effective length has been estimated for different specimen dimensions and materials, as well as for different heating rates. The obtained results suggest that an optimization of experimental parameters, such as the specimen diameter, specimen total and effective length and heating rate, is needed for minimization of the temperature non-uniformity effect.

Key words: *heat conduction, heat radiation, high temperatures, pulse calorimetry, thermophysical properties*

Introduction

The first direct electrical heating of a specimen in the form of a wire based on the measurement of stored energy was carried out by Worthing [1] in 1918. Much later, Nathan [2] applied an elevated heating rate in order to reduce possible chemical reactions, mechanical stress and minimize the effect of conduction due to nonuniform temperature distribution along the specimen at high temperatures. This author used a heating rate of 1000 K/s and recorded the transient specimen temperature using a 0.1 mm spot-welded Pt/Pt13%Rh thermocouple. The same principle was then applied by Kollie [3], who introduced a fast digital data acquisition system for simultaneous measurement of related experimental signals and correction of experimental data, later confirmed by Dobrosavljević and Maglić [4] using another experimental facility based on this work. With the development of radiation non-contact thermometry, an even faster heating rate was introduced by Cezairliyan *et al.* [5]. They introduced a fast photoelectric pyrometer and a tube-shaped specimen with a tiny centered hole through which radiation passed towards the detector. The absolute specimen temperature in this case was measured as the radiance temperature emitted by the black body from a small hole made in the center of the tubular specimen.

* Corresponding author, e-mail: ivanaal@vinca.rs

Although the rise of the heating rates minimizes the heat conduction effect, the temperature distribution across the specimen diameter and along the specimen length remains always nonuniform due to inevitable radiation at high temperatures and existing boundary conditions at the specimen ends being kept at a low temperature. A quantitative study of this temperature nonuniformity is possible only by using some numerical means, such as FEM analysis. Thus, based on the theoretical work of the heat diffusion in presence of electrical current by Barta [6], first simulations of the pulse heating technique and corresponding analysis of the temperature distribution were made by Spišiak *et al.* [7]. They considered a tungsten specimen in the form of a thick and a long cylinder, assuming a finite temperature gradient across the specimen diameter and zero temperature gradient along the specimen length. By taking tungsten and titanium as examples of high and low thermal conductivity materials, Kaschnitz and Supancic [8] studied temperature distribution in a tubular specimen with a centered hole, which was used in practice for noncontact temperature measurements. They assessed a temperature nonuniformity across the specimen diameter, but particularly found a significant temperature distortion in the vicinity of the hole. In order to minimize the latter effect, these authors suggested an optimization of both the tube and hole dimensions. The initial work of Spišiak *et al.* [7] was continued by Bussolino *et al.* [9], where they applied a numerical model on the cylindrical tungsten specimen, for three different specimen diameters and for a constant specimen length, also under assumption of temperature uniformity along the specimen length. Later, Bussolino and Righini [10] applied the same model on the tubular specimen, but used two different heating rates and included thermal expansion for the analysis of the temperature distribution per cross-section of the sample.

In order to further investigate the temperature non-uniformity of the wire-shaped sample using the current pulse method, in this work the temperature distribution was analyzed across the cross-section of the sample as well as along the sample within the effective measurement zone. First, a model that corresponds to boundary and transient conditions similar to those found in experimental condition has been created in COMSOL® Multiphysics software. Then, the model has been validated using the recent high temperature experimental data on a tungsten specimen [11] and, finally, applied for studying the temperature distribution across and along the specimen at different heating rates, specimen diameters and length, as well as for three different materials, tungsten, molybdenum and tantalum. Results of the study are presented and discussed in this paper.

Model and verification

Model

The principle of the pulse calorimetry technique is: A rod shaped specimen of the material under test is heated by electrical current during a short period of time and let to be freely cooled afterwards. The ends of the specimen are hold at the ambient temperature, T_0 . The transient temperature at the central location of the specimen surface, T_c , is measured by thermocouple or radiation thermometer. Data on the specimen current, i , voltage drop across the specimen effective length, u_{eff} , and temperature of the specimen center, T_c , are simultaneously recorded during the heating and the beginning of the cooling period and subsequently used for the determination of the specimen thermophysical properties, such as the specific heat and specific electrical resistivity.

Mathematical description of this principle is given by the heat diffusion equation in electrical conductors [6]:

$$\delta c_p \frac{\partial T}{\partial t} = \nabla k \nabla T + \mu j \nabla T + \rho j^2 \quad (1)$$

where T , t , δ , c_p , k , and ρ are temperature at any specimen point, time, density, specific heat, thermal conductivity, and specific electrical resistivity of the specimen material, while μ and j are the Thomson coefficient and electrical current density through the specimen, respectively. At the beginning of the heating period, the specimen temperature is equal to that of the ambient and at the end of the same period starts the specimen cooling. Boundary conditions at the specimen lateral surface (radial direction, r) is defined by the Fourier and Stefan-Boltzmann law:

$$-k c_p \frac{\partial T}{\partial r} = \varepsilon_{\text{th}} \sigma (T^4 - T_0^4), \quad r = R \quad (2)$$

where R , ε_{th} , and σ are the specimen radius, total hemispherical emissivity of the specimen surface, and Stefan-Boltzmann constant, respectively, while boundary conditions at the specimen two base surfaces (axial direction, x) are those of the first, Dirichlet type:

$$T = T_0, \quad x = 0, L \quad (3)$$

where L is the specimen length. Equations (1)-(3) coupled with the Maxwell equations, which describe electrical field and current density, represent the model used in this work.

A model having this principle was created by using the COMSOL[®] Multiphysics software. The input parameters of the model were the specimen dimensions at ambient temperature, all the related temperature-dependent thermophysical properties of the specimen material (specific heat, thermal conductivity, specific electrical resistivity, total hemispherical emissivity, the coefficient of thermal expansion and density) and the time-dependent DC current which passes through the specimen. On the other hand, application of the model gave the temperature values within the entire specimen volume, voltage drop across the specimen effective length, as well as the specimen length and diameter variation due to the corresponding thermal expansion.

Verification

In order to verify the model, simulations were performed using the measured data and parameters from a recent experiment made on a pure polycrystalline tungsten specimen [11]. The specimen was 3.43 mm in diameter, 200.7 mm in length, and 19.27 g/cm³ in density. The heating time durations were from 900 ms to 2 seconds, with the constant time step of 1 ms. As input parameters in simulations, the directly measured data on DC current was used, as well as the following thermophysical properties of tungsten taken from the literature: the specific heat, specific electrical resistivity and total hemispherical emissivity from [11], thermal conductivity from [12], and the coefficient of thermal expansion from [13]. In the same way as in real experiments, the thermal stress of the specimen was simulated by fixing its one end and leaving the rest free to expand in all directions, while the effective specimen length, symmetrically located from the specimen center and over which the voltage drop and temperature distribution were computed, was 20 mm at ambient temperature.

Simulation data and their comparison with typical experimental signals are given in fig. 1. A good coincidence can be observed, both in the temperature and voltage drop values. Slight difference in data can be seen at higher temperatures only, which is the consequence of using the averaged functions of the specimen thermophysical properties based on measurement data in simulations.

As the validity of the model was verified, temperature non-uniformity along and across the specimen could be studied. As an example, using the same input parameters and

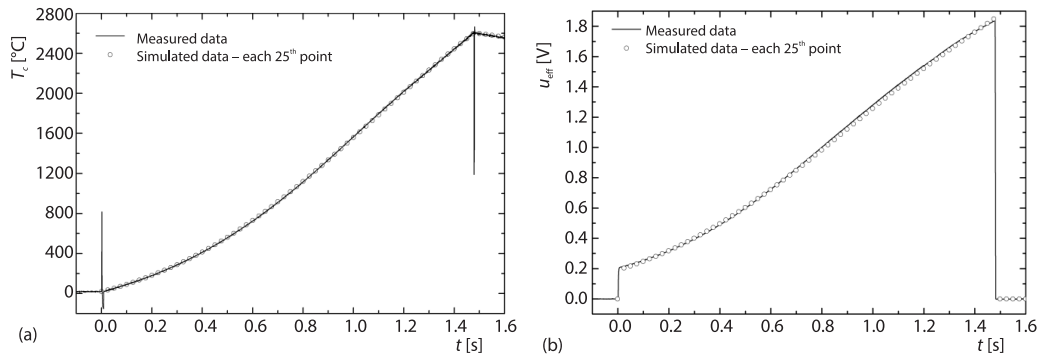


Figure 1. Comparison between measured and simulated data during the specimen heating; (a) surface temperature of the specimen center and (b) voltage drop across the specimen effective length

specimen material, temperature distributions in two directions during the specimen heating are shown in fig. 2. It can be seen that, in this case, the temperature distribution in axial direction is far more uniform than that in the radial direction, which confirms, in general, the validity of a long wire approximation used in previous studies [7-10]. In this work, however, simulations were performed for short and thick specimens and for three different materials and the corresponding results are presented in the next section.

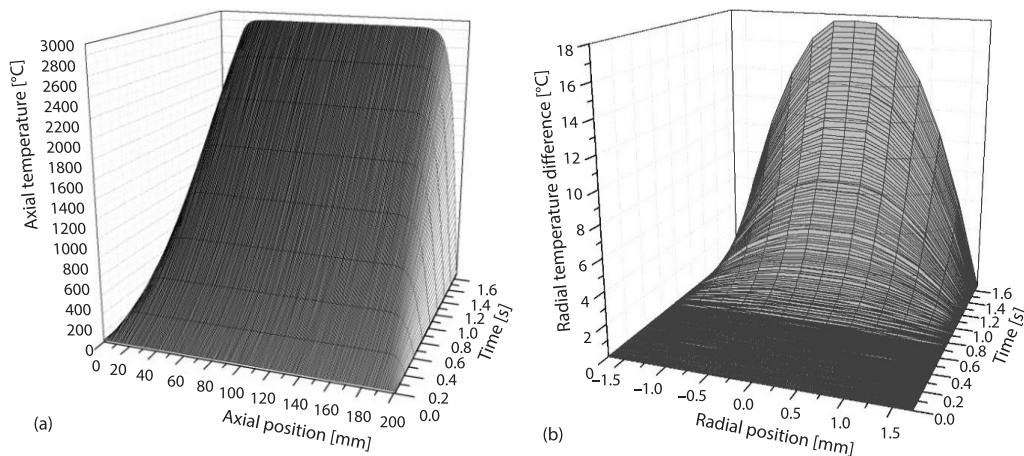


Figure 2. Temperature non-uniformity during the specimen heating in the case of a long specimen used for the verification; (a) along and (b) across the specimen

Results and discussion

In order to investigate the temperature distribution in the specimen in both axial and radial directions, simulations have been performed for different heating rates, specimen diameters of 1 mm, 3 mm, and 5 mm, total specimen lengths of 50 mm, 60 mm, and 80 mm and for specimen materials of tungsten, tantalum, and molybdenum. The effective specimen length was kept constant at the typical value of 20 mm. As for tungsten in the previous section, input data for tantalum and molybdenum thermophysical properties are taken from literature, the specific heat, specific electrical resistivity and total hemispherical emissivity from [14] for tantalum and

from [15] for molybdenum, while thermal conductivity and the coefficient of thermal expansion from [12, 13], respectively, for the both materials. The radial temperature non-uniformity, ΔT_{rad} , represented the maximum temperature difference across the central specimen cross-section, while the axial temperature non-uniformity, ΔT_{ax} , implied the maximum temperature difference on the specimen surface along the specimen effective length. For the sake of comparison, only the data of the temperature distribution at 2500 °C were taken for analysis.

Therefore, results of simulations on the temperature non-uniformity across the specimen in function of the heating rate, r , and for three specimen diameters and three specimen materials are given in fig. 3. It can be seen that for the smallest specimen diameter, the radial temperature non-uniformity is smallest, regardless the heating rate and the specimen material. It increases almost linearly for thicker specimens, but decreases slowly with the heating rate rise. Concerning the material, the radial non-uniformity is highest for tantalum, which is expected as its total hemispherical emissivity is much higher at 2500 °C than that of tungsten and molybdenum. Overall, according to these results, the effect of the radial non-uniformity can be neglected only in thin specimens, which is in agreement with the aforementioned studies, while the influence of the heating rate seems to be not significant for this temperature distribution.

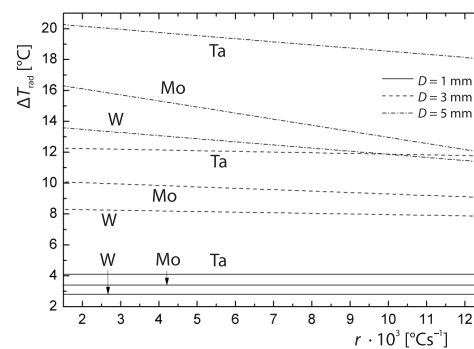


Figure 3. Temperature non-uniformity across the specimen at 2500 °C in function of the heating rate for different specimen diameters and materials

On the other hand, the results of the temperature non-uniformity along the specimen effective length, also in function of the heating rate and for different specimen diameters, lengths and materials, are shown in fig. 4. According to them, two first clear outcomes are seen: the axial temperature non-uniformity dramatically rises with the decrease of the total specimen length and the same non-uniformity equally falls with the rise of the heating rate, regardless the specimen diameter and material. The former means the longer the total specimen length, the better the temperature uniformity along the specimen effective length and there is a critical total specimen length, let us say 80 mm in these examples, below which this uniformity dramatically worsens. The other outcome reveals that even in the case of the shortest total length, the axial temperature non-uniformity practically disappears with a sufficient mounting of the heating rate.

The results presented in fig. 4 also show that the level of axial temperature non-uniformity is influenced by the specimen diameter and material. A lower diameter generally means a better axial uniformity, which, having the same effect on the radial uniformity, completely justifies approximation of a thin and long wire used by the previous authors. For higher diameters, however, the temperature non-uniformity along the specimen effective length may rise significantly, as it is shown in fig. 4. Concerning the specimen material, the axial temperature non-uniformity is most affected by the material's thermal conductivity and thermal diffusivity. As of three selected materials tungsten has the highest and tantalum the lowest value of thermal conductivity at 2500 °C, so the order of the axial temperature non-uniformity for these three materials is equivalent to the same specimen diameter and the heating rate.

The results presented in fig. 4 also show that the level of axial temperature non-uniformity is influenced by the specimen diameter and material. A lower diameter generally means a better axial uniformity, which, having the same effect on the radial uniformity, completely justifies approximation of a thin and long wire used by the previous authors. For higher diameters, however, the temperature non-uniformity along the specimen effective length may rise significantly, as it is shown in fig. 4. Concerning the specimen material, the axial temperature non-uniformity is most affected by the material's thermal conductivity and thermal diffusivity. As of three selected materials tungsten has the highest and tantalum the lowest value of thermal conductivity at 2500 °C, so the order of the axial temperature non-uniformity for these three materials is equivalent to the same specimen diameter and the heating rate.

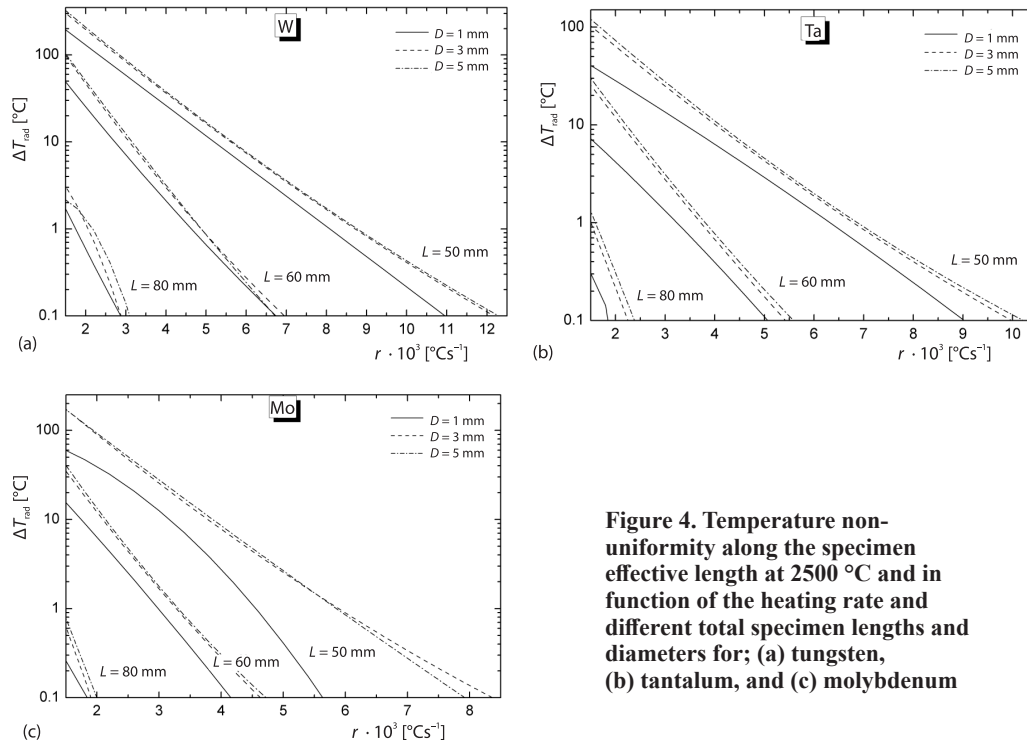


Figure 4. Temperature non-uniformity along the specimen effective length at 2500 °C and in function of the heating rate and different total specimen lengths and diameters for; (a) tungsten, (b) tantalum, and (c) molybdenum

All the results, for both radial and axial temperature distributions, reveal a strong and complex dependence between the temperature non-uniformity during the specimen heating from one side and specimen dimensions, various thermophysical properties of the specimen material and experimental parameters, such as the heating rate and specimen effective length, from the other side. In practice, the properties of the specimen material are normally unknown, need to be determined and cannot be modified. Therefore, in order to minimize the temperature non-uniformity across and along the specimen in the pulse calorimetry technique, the specimen dimensions, heating rate and specimen effective length should be optimized.

An effective approach for this optimization is, certainly, the use of thin and long specimens. However, such the specimens may have too high electrical resistance, which may, in turn, require a high DC power source for heating the specimen rapidly. The same requirement will be in the case of rising the heating rate. Moreover, too high heating rates imply the use of temperature sensors with a very high responsivity, which is difficult to achieve with the contact thermometry. Finally, the specimen effective length may be reduced in order to make the temperature non-uniformity less important, but such a reduction has also limits because it may produce a significant loss of the signal-noise ratio of the voltage drop measurement, as well as an important increase of the uncertainty of the obtained thermophysical properties, specific heat and specific electrical resistivity. Therefore, in each specific application of the pulse calorimetry technique, *i.e.*, for each specimen material and its dimensions and expected properties, one should perform a corresponding simulation, estimate the value of the radial and axial temperature non-uniformity and set the experimental parameters, heating rate and specimen effective length, in order to minimize the effect of the non-uniform temperature distribution on the final measurement results.

Conclusion

Standard application of the pulse calorimetry technique assumes conditions of a uniform temperature distribution across the specimen diameter and along the specimen effective length. Such conditions are usually satisfied in practice in the cases of heating thin and long specimens. By using FEM simulations in COMSOL® Multiphysics, the results of virtual experiments reveal that the level of the temperature non-uniformity in both the radial and axial specimen direction for different specimen dimensions and materials, as well as for different heating rates, significantly varies. While the temperature non-uniformity across the specimen diameter linearly increase with the rise of the specimen thickness, the non-uniformity along the specimen effective length may dramatically rise with the decrease of the specimen total length. Also, both the radial and, especially, axial temperature non-uniformity are reduced with the heating rate mounting. Therefore, in order to reduce the effect of a non-uniform temperature distribution for relatively thick and short specimens, it is necessary to perform corresponding numerical analysis and optimize experimental parameters, such as the heating rate and specimen effective length.

Acknowledgment

This work has been performed under research topic number 1402202 of the Institute VINČA. The research has been funded by the Ministry of Education, Science and Technological Development of the Republic of Serbia.

Nomenclature

c_p – specific heat, [Jkg⁻¹K⁻¹]
 i – specimen current, [A]
 j – electrical current density through the specimen, [Am⁻²]
 k – thermal conductivity, [Wm⁻¹K⁻¹]
 L – the specimen length, [mm]
 R – the specimen radius, [mm]
 r – radial direction
 T – temperature at any specimen point, [°C]
 ΔT – temperature non-uniformity, [°C]
 t – time, [s]
 u – voltage drop across the specimen, [V]
 x – axial direction

Greek symbols

δ – density, [kgm⁻³]
 ϵ_{th} – total hemispherical emissivity of the specimen surface
 μ – Thomson coefficient, [KMPa⁻¹]
 ρ – electrical resistivity of the specimen material, [Ω m]

Subscripts

ax – axial direction
c – central location of the specimen surface
eff – effective domain
rad – radial direction

References

- [1] Worthing, A. G., Atomic Heats of Tungsten and of Carbon at Incandescent Temperatures, *Phys. Rev.*, 12, (1918), 3, pp. 199-225, 1918
- [2] Nathan, A. M., A Dynamic Method for Measuring the Specific Heat of Metals, *Journal Appl. Phys.*, Vol., 22 (1951), p. 234-235
- [3] Kollie, T., Specific Heat Determinations by Pulse Calorimetry Utilizing a Digital Voltmeter for Data Acquisition, *Rev. Sci. Instr.*, 38 (1967), 10, pp. 1452-1463
- [4] Dobrosavljević, A. S., Maglić, K. D., Pulse Heating Method for Specific Heat and Electrical Resistivity Measurement in the Range 300-1400 K, in: *Advanced Course in Measurement Techniques in Heat and Mass Transfer*, (Eds. Soloukhin R. I. and Afgan, N.), Hemisphere, Washington DC, USA, 1985, pp. 411-420
- [5] Cezairliyan, A., *et al.*, High-Speed (subsecond) Measurement of Heat Capacity, Electrical Resistivity, and Thermal Radiation Properties of Molybdenum in the Range 1900-2800 K, *Journal Res. Natl. Bur. Stand.*, 74A (1970), 1, pp. 65-92
- [6] Barta, Š., Thermodiffusion and Thermo-Electric Phenomena in Condensed Systems, *Int. J. Heat Mass Transf.*, 39 (1996), 16, pp. 3531-3542

- [7] Spišiak, J., *et al.*, Mathematical Models for Pulse-Heating Experiments, *Int. J. Thermophys.*, 22 (2001), 4, pp. 1241-1251
- [8] Kaschnitz, E., Supancic, P., The 3-D Finite-Element Analysis of High-Speed (Milisecond) Measurements, *Int. J. Thermophys.*, 26 (2005), 4, pp. 957-967
- [9] Bussolino, G. C., *et al.*, Virtual Experiments by Pulse Heating Techniques: Cylindrical Tungsten Specimens, *Int. J. Thermophys.*, 32 (2011), Oct., pp. 2716-2726
- [10] Bussolino, Righini, F., Virtual Experiments by Pulse Heating Techniques: Tubular Tungsten Specimens, *Int. J. Thermophys.*, 34 (2013), Mar., pp. 78-92
- [11] Milošević, N. D., Application of the Subsecond Calorimetry Technique with Both Contact and Radiance Temperature Measurements: Case Study on Solid Phase Tungsten at Very High Temperatures, *Journal Thermal Analys. Calorim.*, (2022), 147, pp. 4935-4943
- [12] Touloukian, Y. S., *et al.*, *Thermophysical Properties of Matter; Thermal Conductivity, Metallic Elements and Alloys*, IFI/Plenum: New York, USA, 1970., Vol. 1
- [13] Touloukian, Y. S., *et al.*, *Thermophysical Properties of Matter; Thermal Expansion – Metallic Elements and Alloys*, IFI/Plenum: New York, USA, 1975, Vol. 12
- [14] Milošević, N. D., *et al.*, Thermal Properties of Tantalum Between 300 and 2300 K, *Int. J. Thermophys.*, 20 (1999), 4, pp. 1129-1136
- [15] Maglić, K. D., *et al.*, Specific Heat and Specific Electrical Resistivity of Molybdenum between 400 and 2500 K, *High Temp. High Press.*, 29 (1997), pp. 97-102